JOURNAL OF MATERIALS SCIENCE 29 (1994) 4834–4839

Synthesis and characterization of tungsten disulphide films grown by pulsed-laser deposition

J. S. ZABINSKI*, M. S. DONLEY, S. V. PRASAD
Wright Laboratory, Materials Directorate (WL/MLBT), Wright-Patterson Air Force Base, OH 45433, USA

N. T. McDEVITT
RAMSPEC Research, 4399 E. Mohave Drive, Dayton, OH 45431, USA

The synthesis and characterization of tungsten disulphide (WS_2) films grown on 440C stainless steel substrates using the 248 nm line from a KrF excimer laser are reported. Film properties could be adjusted by controlling substrate temperature and by laser or thermal anneals. X-ray photoelectron spectroscopy, glancing angle XRD, Raman spectroscopy and high-resolution scanning electron microscopy were used to evaluate film chemistry, crystallinity and morphology. Films grown at room temperature were amorphous, near stoichiometric, and had a multiplicity of chemical states. Local order and bonding were improved most dramatically through post-deposition laser anneals. Crystallite size could be increased by raising the substrate temperature during deposition and, to a lesser degree, by post-deposition thermal anneals. Local disorder was observed within the larger crystallites compared to those that were laser annealed. Crystallinity was induced in amorphous films by mechanical rubbing at room temperature under conditions where frictional heating was negligible. The degree of control over film properties provided by PLD demonstrates its value for growing/designing tribological coatings.

1. Introduction

Tungsten disulphide (WS_2) is a solid lubricant from the class of compounds known as transition metal dichalcogenides. These materials typically have a hexagonal crystal structure which is composed of two-dimensional sheets stacked on top of one another. Each sheet is tri-layered with a metal atom (e.g. Mo, W, Nb or Ta) in the middle that is covalently bonded to chalcogen atoms (e.g. S, Se or Te) in the top and bottom layers. The covalently bonded sheets are held together by weak Van der Waals forces which permits them to shear easily. The basal plane is composed of a layer of chalcogen atoms which are quite inert, permitting easy intercrystalline slip. The crystal structure and the inertness of the basal plane are responsible for the low-friction surface and high load-carrying capability of the transition metal dichalcogenides [1]. These materials have been used successfully in a variety of technological applications and in a number of different forms: (1) as part of a bonded coating, (2) as part of a compact, (3) as a burnished film, (4) as a sputtered film, and (5) as a laser-deposited film.

Molybdenum disulphide (MoS_2) is the most used and most frequently studied transition metal dichalcogen lubricant. It provides an ultra-low friction surface ($0.008 < \mu < 0.05$) and long wear life in dry environments and vacuum; the presence of moisture severely curtails its wear life by several orders of magnitude and causes a rise in the friction coefficient to 0.1–0.2. Tungsten disulphide is nearly a direct replacement for MoS_2 because it has very similar properties. However, WS_2 is more resistant to oxidation at elevated temperature providing about a 100 °C increase in maximum operating temperature [2]. Because MoS_2 is a naturally occurring mineral and WS_2 is a synthetic material, MoS_2 has been used much more frequently.

The general trend for improving advanced solid lubricants is to increase their life at high temperature. For aerospace applications, lubricant films are also required to be thin and of uniform thickness. Therefore, it is critical to develop precision film growth techniques for high-temperature lubricants. Pulsed laser deposition (PLD) has been employed successfully to grow high-quality films that are fully dense, long lasting, and have low friction surfaces. Film properties such as crystallinity, stoichiometry, morphology and dopant concentration can easily be adjusted by varying PLD parameters [3–6]. Because it is exactly these properties that are important for determining tribological behaviour, PLD is an ideal technique for tailoring film properties to different tribological applications.

The feasibility of using PLD to grow WS_2 films has been evaluated elsewhere [7]. Films evaluated for that study were grown on aluminium metal-matrix com-

---

* Author to whom all correspondence should be addressed.

0022–2461

posites at 350 °C; they were dense, near stoichiometric, and exhibited a low friction coefficient of around 0.04. The objective of this study was to give a detailed account of the synthesis of WS_2 by PLD and to evaluate the role of substrate temperature, laser anneals, and thermal anneals on the chemistry and crystallinity of the films. It was reported earlier that such parameters have a profound influence on PLD film properties [3–6]. Because the WS_2 films are targeted for use as tribological coatings, 440C tempered stainless steel discs were selected as substrates (hardness = 60 HRC; $R_a = 4.7$ nm). X-ray photoelectron spectroscopy (XPS), glancing angle XRD (GAXRD), Raman spectroscopy and scanning electron microscopy (SEM) were used to evaluate chemistry, crystallinity and morphology.

2. Experimental procedure

A stainless steel vacuum chamber having a base pressure of 8×10^{-7} Pa was used for film deposition; the pressure during deposition rose to 1×10^{-5} Pa. A more detailed description of the procedures for PLD of lubricant materials is available in earlier reports [3, 6, 8, 9]. Tungsten disulphide targets were fabricated by cold pressing WS_2 powder (Aldrich Chemical 99.8% pure) into 25 mm diameter discs at 50 MPa.

A Lambda Physik LPX 110i excimer laser charged with KrF was used to provide 248 nm radiation to the target. The laser was set for 100 mJ/pulse and 25 Hz; it was focused to a 2.0 mm by 4.5 mm rectangle on the target face which provided a fluence of 1.1 J cm^{-2}. The unfocused laser beam (38 mJ cm^{-2}) was used for post-deposition anneals which were done in air. Film uniformity was maximized by: (1) rotating the target and the substrate at about 10 r.p.m during deposition and (2) rastering the laser beam across the target face. A calibrated quartz crystal oscillator was used to measure deposition rates and film thicknesses. Resistive heating was employed to degas and/or anneal the specimens; temperature was measured using a calibrated infrared pyrometer. Targets were polished with a lint-free cloth to minimize target roughness and increase deposition rates; they were preconditioned by ablative cleaning for 5 min prior to film growth using the focused laser beam. The sample shutter was closed during target cleaning.

2.1. Sample preparation and analysis

Substrates were fabricated from 440C stainless steel (SS) coupons (60 HRC) that were polished to 0.01 μm and cleaned ultrasonically in acetone, methanol and water. Prior to deposition, the specimens were degased at 300 °C for 15 min and allowed to cool to room temperature. The duration of each deposition was adjusted to provide films that were about 600.0 nm thick. Clean and degassed substrates were coated at room temperature and at 350 °C. Films grown at room temperature were subjected to (1) 2 min laser annealing, and (2) 15 min thermal annealing at 350 °C.

Surface chemistry was studied with a Surface Science Instruments (SSI) M-probe XPS instrument operated at 3×10^{-7} Pa using a 200 × 1000 μm line spot and a 25 eV pass energy to provide a full-width half-maximum (FWHM) of 0.71 eV for the Au $4f_{7/2}$ peak. Binding energy positions were calibrated using the Au $4f_{7/2}$ peak at 84.0 eV, and the Cu 3s and Cu $2p_{3/2}$ peaks at 122.39 and 932.47 eV, respectively. Bulk chemistry and film crystallinity were investigated by Raman spectroscopy using a SPEX 1877 spectrometer and the incident light of a 514.5 nm argon ion laser. An intensified 1024 element, diode array detector was used to collect the Raman signal. Film crystal structures were determined using data acquired by a Rigaku D/max-1B diffractometer equipped with a thin-film attachment and a monochrometer. WS_2 powder and film morphologies were evaluated using a Jeol 840F scanning electron microscope equipped with energy and wavelength dispersive X-ray spectroscopes.

3. Results and discussion

3.1. Morphology

The morphology of WS_2, as it was pressed into a pellet, laser ablated and then condensed as a film, was observed using high-resolution SEM. Fig. 1a shows the powdered WS_2 before it was pressed. The largest dimension of the individual particles is along the basal plane surface and, as a consequence of their lamellar crystal structure, they are shaped like platelets. The platelet faces are the low-energy sulphur-terminated basal planes. After pressing, the fresh target has a relatively smooth surface as illustrated in Fig. 1b. Ablating the target causes its surface to become textured, which is well known in the field. The topography of the ablated target can best be described as being cone-like (Fig. 1c). A typical film grown at room temperature is shown in Fig. 1d; the film is nearly fully dense and its surface has a "cauliflower" appearance. Particles like these are frequently observed in PLD films; they originate from subsurface vaporization and subsequent ejection of molten material. Mechanical ejection of small particles may also contribute to the particle density. A film grown at 350 °C is shown in Fig. 1e and is noticeably different; it is powdery, porous and appears to have larger crystals than the RT films.

3.2. Chemistry

The chemical bonding in the different films was evaluated by X-ray photoelectron spectroscopy. Fig. 2 shows the W 4f and S 2p photoelectron peaks arising from the films as well as those from the target for comparison. XPS data were fit using Voight functions and the resulting peak parameters are listed in Table I. The most significant observation is that film chemistry correlates with increasing energy input, either by increasing the temperature of the substrates during deposition, post-deposition thermal anneals or post-deposition laser anneals. The RT film provides broad photoelectron peaks which are shifted to lower binding energy compared to the target. Peak broadening is evidence of disorder and a multiplicity of chemical

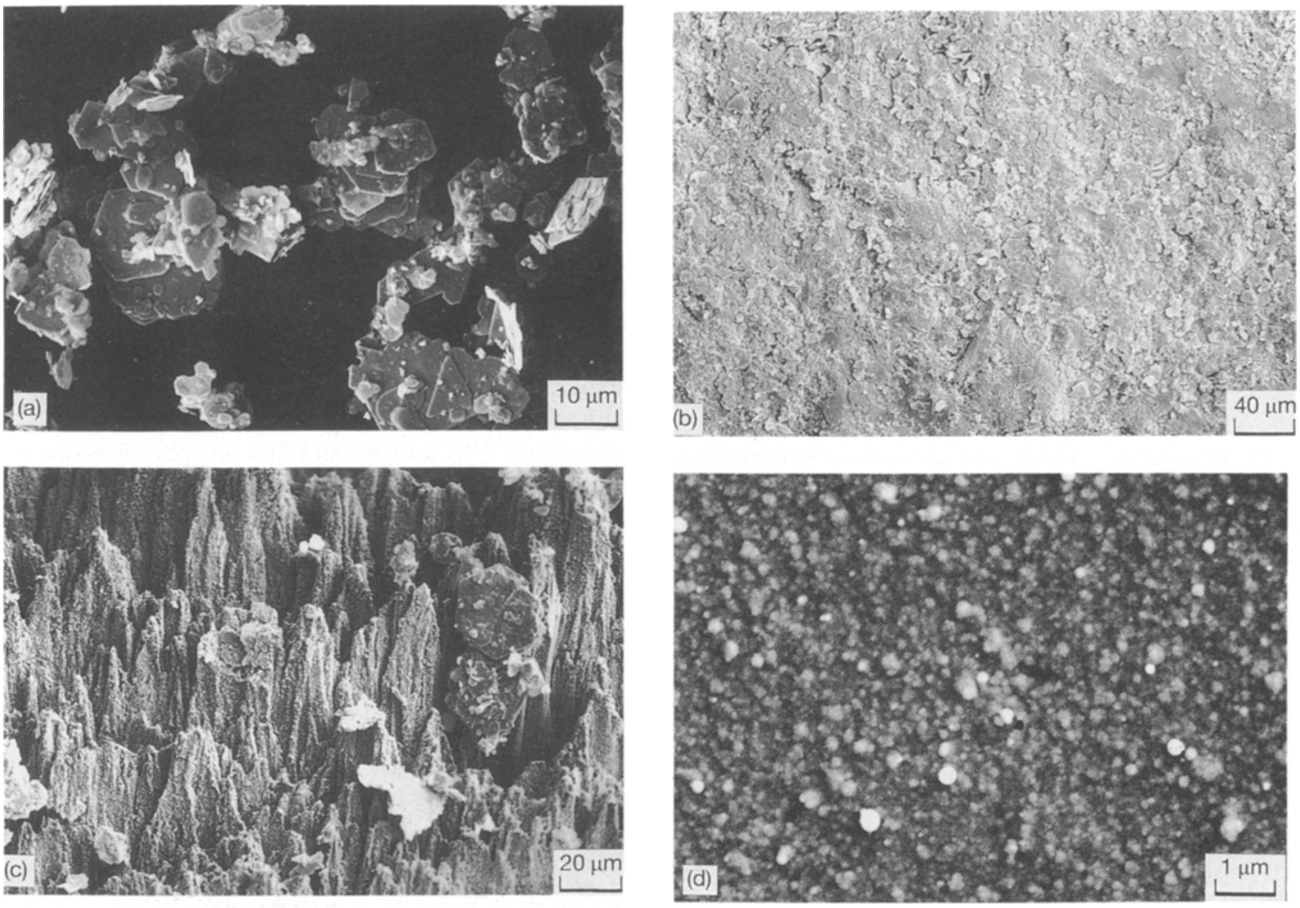

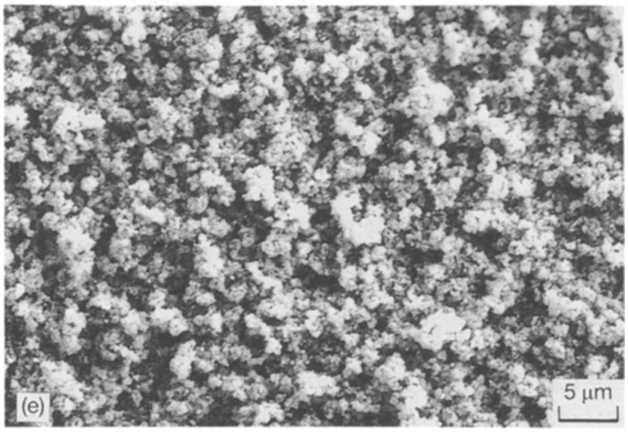

Figure 1 Scanning electron micrographs showing (a) WS_2 powder, (b) a pressed target of the WS_2 powder in (a), (c) laser-ablated target, (d) WS_2 film grown at room temperature, and (e) WS_2 film grown at 350 °C.

states. A shift to lower binding energy is typical of disordered MoS_2 films. In the case of MoS_2, band bending has been suggested as the origin of the phenomenon [10]. Because the crystal structures and properties of MoS_2 and WS_2 are similar, the same explanation may apply to WS_2 as well.

The energy separation of the W $4f_{7/2}$ and S $2p_{3/2}$ peaks for all treated films is nearly identical to that in the target (films – 129.62 ± 0.01 eV; target = 129.58 eV). The energy separation in as-deposited room-temperature films is 129.45 eV; this reflects some difference in chemical binding but it is noted the XPS peaks from this film were broad and difficult to fit. Binding energy, W–S binding energy separation and film stoichiometry were used to identify the major component in the films as WS_2. Raman and XRD data, discussed later, support that assignment. Films were transferred in air causing some oxidation (WO_3)

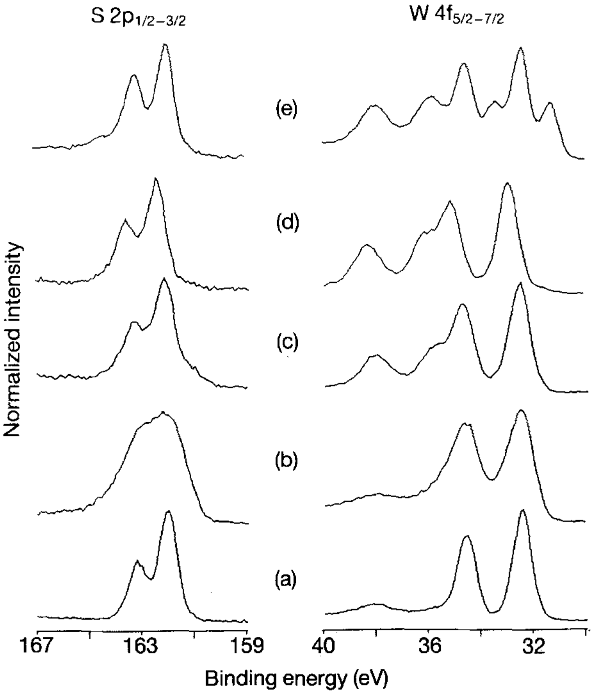

Figure 2 X-ray photoelectron spectra of the W $4f_{5/2-7/2}$ and S $2p_{1/2-3/2}$ doublets from (a) the WS_2 target, (b) the film grown at room temperature, (c) the film grown at 350 °C, (d) the film grown at RT and annealed at 350 °C for 15 min, and (e) the film grown at room temperature and laser annealed for 15 min.

TABLE I XPS data from the WS_2 target, the RT film, the film grown at 350 °C, the film grown at RT and annealed at 350 °C for 15 min, and the film grown at room temperature and laser annealed for 15 min.

Specimen	WS_2				S^0	S?	WO_3	W^0
	W $4f_{7/2}$	S $2p_{3/2}$	S/W	S − W	S $2p_{3/2}$	S $2p_{3/2}$	W $4f_{7/2}$	W $4f_{7/2}$
Target	32.96	162.54	2.00	129.58	–	–	36.23	–
RT	32.40	161.85	1.96	129.45	163.05	–	35.77	–
350 °C	32.68	162.30	1.75	129.62	163.08	161.25	35.85	31.25
RT and TA	32.17	161.78	2.06	129.61	–	160.69	35.50	–
RT and LA	32.50	162.13	1.94	129.63	163.38	161.10	35.93	31.36

as evinced by the second doublet to higher binding energy observed in the W 4f spectra. Laser annealing an RT film in air caused the formation of significant amounts of metallic tungsten as shown by the W $4f_{7/2}$ peak at 31.36 eV in addition to WO_3 and WS_2; the film grown at 350 °C also has a small quantity of metallic tungsten (W $4f_{7/2} = 31.48$ eV). Two types of sulphur were observed in the RT film: elemental sulphur and sulphur chemically bonded as WS_2. The elemental sulphur is most likely concentrated on the film surface where it condensed after deposition. Measurements from a residual gas analyser (RGA) confirm that sulphur vapour is persistent in the chamber for some time after deposition. Sulphur has a relatively high vapour pressure which explains this phenomenon. Similar observations have been made for PLD MoS_2 films and XPS/RBS data demonstrated that elemental sulphur was concentrated at the surface for this system [3]. A fraction ($< 9\%$) of a third type of sulphur (not assigned to a compound) was observed in the treated films appearing at about 161.30 eV.

As shown in Fig. 2, thermal and laser treatments reduced the disorder and chemical multiplicity in the films. XPS data show this by the narrowing of the peak FWHMs. In addition, the concentration of elemental sulphur decreased significantly after treatments compared to the as-deposited RT film. The energy input to the specimens caused the sulphur to desorb from the film surface; again, this has been observed with PLD MoS_2 films [3]. Raman peaks shown in Fig. 3 confirm the XPS data: RT films are amorphous while thermal and laser anneals improve chemical bonding and film crystallinity.

3.3. Crystal structure

Raman spectroscopy and GAXRD were used to measure film crystallinity; Figs 3 and 4 show the Raman and XRD data. The as-deposited RT film provides featureless spectra for both techniques. This demonstrates that the films are amorphous or have crystalline domains smaller than about 2 nm diameter. Input of thermal or laser energy to a film causes an increase in crystallinity. Raman data (Fig. 3) show the relative order of treatments for increasing crystallinity: 350 °C thermal anneal, 350 °C deposition, post-deposition laser anneal. XRD data shown in Fig. 4 and Table II demonstrate the same ordering for thermal treatments, but the laser-annealed films remain predominantly amorphous. The disagreement between the Raman and XRD data can be understood by considering the range of order required by the two techniques. XRD requires long-range order (greater than about 5–10 nm diameter crystalline domains), whereas Raman is sensitive to shorter range order (~ 2 nm). Laser anneals reduce disorder within a domain and consequently the multiplicity of chemical bonding, but do not cause the crystalline domain size (i.e. the crystallite diameter) to grow. Thermal anneals, however, permit the crystalline domains to nucleate and become larger, thus XRD spectra can be obtained. Crystalline order within the domains is not as high as those within the laser-annealed films.

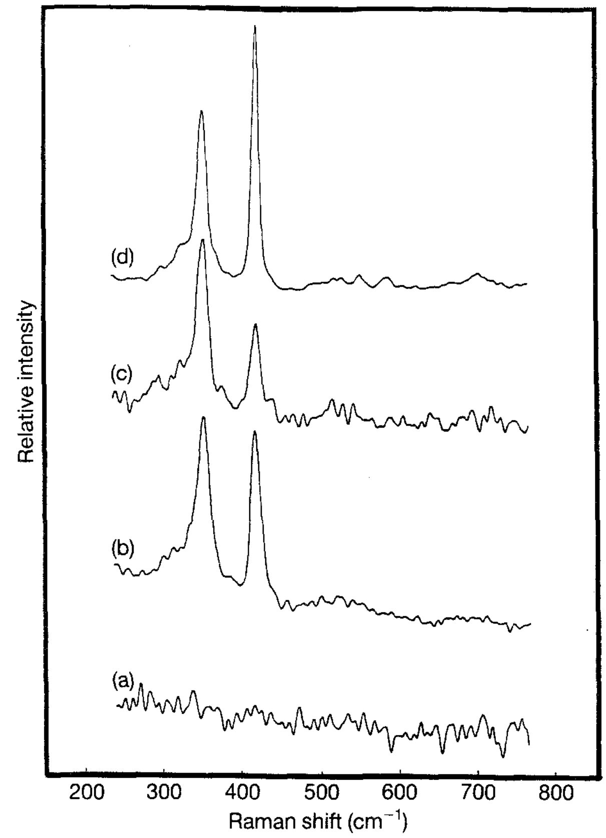

Figure 3 Raman spectra from (a) the film grown at RT, (b) the film grown at 350 °C, (c) the film grown at RT and annealed at 350 °C for 15 min, and (d) the film grown at room temperature and laser annealed.

The tribological properties of the films grown here were evaluated using a ball on disc tribometer. In this test, the friction force exerted on a stationary ball by a rotating disc is monitored as a function of revolutions.

TABLE II Diffraction data from PDF files [11], the film grown at RT and annealed at 350 °C for 15 min, and the film grown at 350 °C

hkl	PDF		Powder		350 °C deposition		350 °C post anneal	
	d (nm)	I/I_1	*d* (nm)	I/I_1	*d* (nm)	I/I_1	*d* (nm)	I/I_1
002	0.618	100	0.6061	100	0.6509	100	0.6553	100
004	0.3089	14	0.3063	4.9	0.31	BB[a]	0.31	BB
100	0.2731	25	0.2712	1.5	0.268	81	0.269	31
101	0.2667	25	0.2650	1.8	0.268	BB	0.269	31
102	0.2498	8	0.2484	0.8	0.2524	12	0.253	26
103	0.2277	35	0.2264	3.9	0.2256	19	0.2252	59
006	0.2061	12	0.2048	2.8	0.2059	12	0.2056	34
105	0.1834	18	0.1824	2.5	–	–	–	–
106	0.1646	2	0.1638	0.4	–	–	–	–
110	0.1578	16	0.1572	0.8	BB	BB	BB	BB
008	0.1546	8	0.1538	1.2	BB	BB	BB	BB
112	0.1529	14	0.1522	0.5	BB	BB	BB	BB
118	0.1104	8	0.1101	1.3	0.1101	1	0.1101	5

[a]BB = broad band

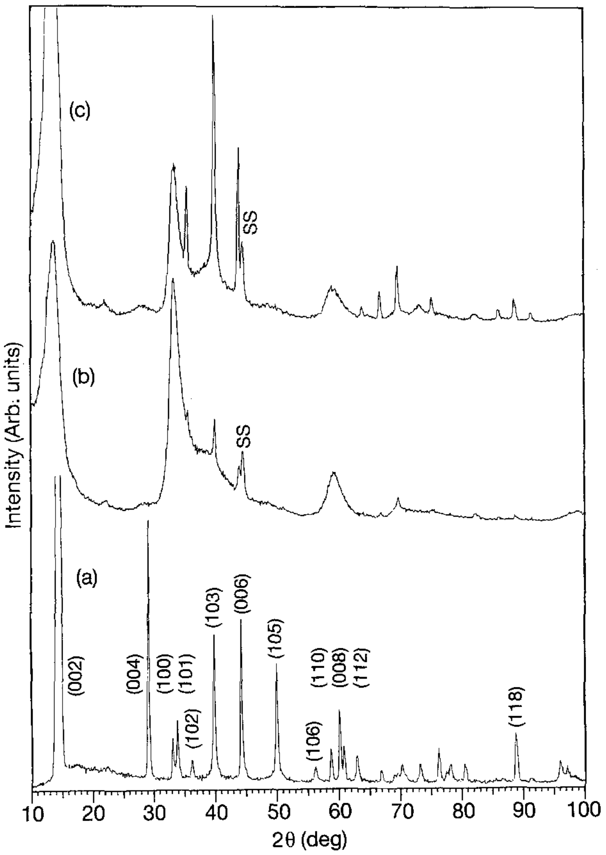

Figure 4 Diffraction patterns collected using GAXRD from (a) the WS_2 powder, (b) the film grown at RT and annealed at 350 °C for 15 min, and (c) the film grown at 350 °C.

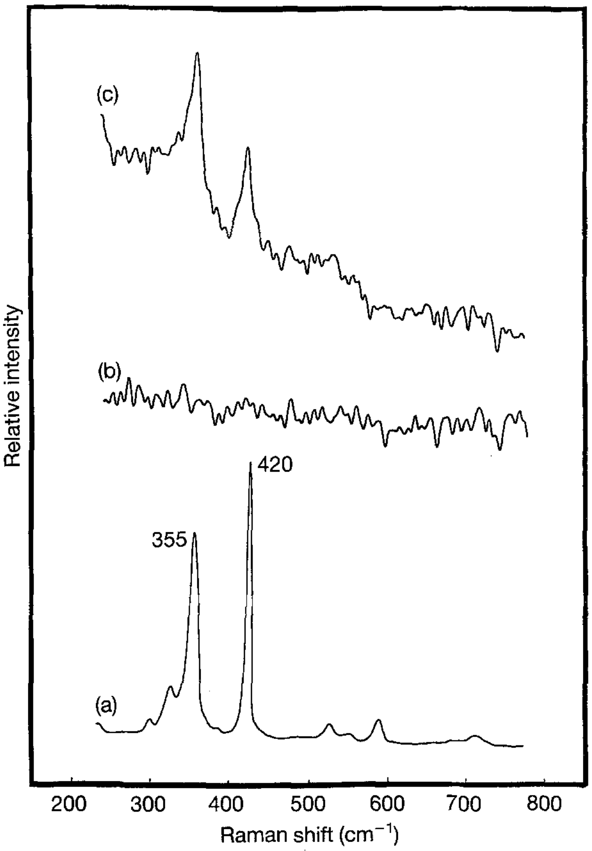

Figure 5 Raman spectra from (a) the crystalline WS_2 powder, (b) the film grown at room temperature, and (c) the wear track of the film shown in (b).

The friction coefficient can be calculated and the wear life of the film is defined as the point where the friction force exceeds a preset value. While the details of those are presented elsewhere [12], the effects of rubbing on crystallinity are briefly discussed. Raman spectra of a film grown at room temperature and then rubbed in a pin-on-disc tribometer are shown in Fig. 5; the Raman spectrum of the target is shown for comparison. Films grown at room temperature are amorphous (Fig. 5b); rubbing in dry nitrogen causes growth of the Raman bands at 355 and 420 cm^{-1} (Fig. 5c) demonstrating crystallization. Energy input to the films by the mechanical action of rubbing causes the films to crystallize just as energy from thermal and laser anneals causes crystallization.

4. Conclusions

PLD was used to grow adherent films of WS_2 on 440C stainless steel substrates. Film chemistry and crystallinity could be adjusted by controlling the substrate temperature and by laser or thermal anneals. Films grown at room temperature are amorphous, near stoichiometric, and have a multiplicity of chemical states. Local order and bonding are improved most dramatically through post-deposition laser anneals. Crystallite size is increased by raising the substrate temperature during deposition and, to a lesser degree, by post-deposition thermal anneals. There is local disorder within the larger crystallites compared to those that were laser annealed. Crystallinity is induced in amorphous films by mechanical rubbing at room temperature under conditions where frictional heating is negligible. The degree of control over film properties provided by PLD demonstrates its value for growing/designing tribological coatings.

References

1. F. J. CLAUSS, "Solid Lubricants and Self-Lubricating Solids" (Academic Press, New York, 1972).
2. H. E. SLINEY, *Tribol. Int.* **15** (1982) 303.
3. J. S. ZABINSKI, M. S. DONLEY, P. J. JOHN, V. J. DYHOUSE, A. SAFRIET and N. T. McDEVITT, in "Surface chemistry and beam-solid Interactions", edited by H. A. Atwater, F. A. Houle and D. H. Lowndes, Materials Research Society Symposium Proceedings, Boston, MA, Vol. 201 (Materials Research Society, Pittsburgh, 1991) p. 195.
4. P. J. JOHN, V. J. DYHOUSE, N. T. McDEVITT, A. SAFRIET, J. S. ZABINSKI and M. S. DONLEY, *ibid.* p. 117.
5. J. S. ZABINSKI, M. S. DONLEY, V. J. DYHOUSE, and N. T. McDEVITT, Thin solid films **214** (1992) 156.
6. *Idem*, in "Photons and Low Energy Particles in Surface Processing", edited by C. I. H. Ashby, J. H. Brannon, and S. W. Pang, Materials Research Society Symposium Proceedings, Boston, MA, Vol. 236 (Materials Research Society, Pittsburgh, 1992) p. 437.
7. S. V. PRASAD, J. S. ZABINSKI and V. J. DYHOUSE, *J. Mater. Sci. Lett.* **11** (1992) 1282.
8. M. S. DONLEY, P. T. MURRAY, S. A. BARBER and T. W. HAAS, *Surf. Coatings Technol.* **36** (1988) 329.
9. M. S. DONLEY, J. S. ZABINSKI, V. J. DYHOUSE, P. J. JOHN, P. T. MURRAY and N. T. McDEVITT, in "Lectures Notes in Physics", Vol. 389, edited by J. C. Miller and R. F. Haglund Jr (Springer, New York, 1991) p. 271.
10. S. V. PRASAD, J. S. ZABINSKI and N. T. McDEVITT, *Tribology Trans*, in press; and *Wear*, to be submitted.
11. J. R. LINCE, D. J. CARRE and P. D. FLEISCHAUER, *Phys. Rev.* **B36** (1987) 1647.
12. Powder Diffraction File: Set 8 (International Centre for Diffraction Data, Swarthmore, PA, 1960) No. 8-237

Received 16 February
and accepted 21 June 1993